Journal of chemical & engineering data

Article

Cite This: *J. Chem. Eng. Data* XXXX, XXX, XXX−XXX

pubs.acs.org/jced

Thermodynamic Characterization of Surface and Solubility of 5-((*S*)-3,7-Dimethyloctyloxy)-2-[[[4-(octyloxy)phenyl]imino]methyl]phenol Liquid Crystal with Some Solvents

Serap Mutlu Yanic,[1] Fatih Cakar,[2] Hale Ocak,[2] Ferdane Karaman,[2] Ozlem Cankurtaran,*[,2] and Belkız Bilgin Eran[2]

[1]Chemistry Technology Programme, Istanbul Gedik University, Pendik Campus, 34906, Istanbul, Turkey
[2]Department of Chemistry, Yildiz Technical University, Davutpasa Campus, 34220, Istanbul, Turkey

Supporting Information

ABSTRACT: The inverse gas chromatography method was used to obtain dispersive surface energy, surface acidity or basicity constants, mole fraction activity coefficients of the solvents at infinite dilution for a new salicylaldimine based chiral calamitic liquid crystal 5-((*S*)-3,7-dimethyloctyloxy)-2-[[[4-(octyloxy)phenyl]imino]methyl]phenol (DOPIMP). The dispersive surface energy of DOPIMP was estimated as 41.1 mJ/m^2 at 30 °C and decreased with temperature. The specific free energy, enthalpy, and entropy of adsorption of the selected polar solvents on the liquid crystal were determined. The values of adsorption enthalpy were correlated with both donor and acceptor numbers of the solvents to quantify acidic K_A and basic K_D parameters of the liquid crystal surface. The results indicated that the surface of DOPIMP is basic. The retention diagrams of *n*-hexane, *n*-heptane, *n*-octane, *n*-nonane, *n*-decane, undecane, ethyl acetate, *n*-butyl acetate, iso-butyl acetate, toluene, ethylbenzene, *n*-propylbenzene, and chlorobenzene on the DOPIMP were plotted as straight lines using the net retention volumes at temperatures between 368.2 and 398.2 K. The values of activity coefficients indicated that DOPIMP was better soluble in long chain alkanes. Negatively signed partial molar Gibbs energies of mixing were obtained at infinite dilution of studied solvents.

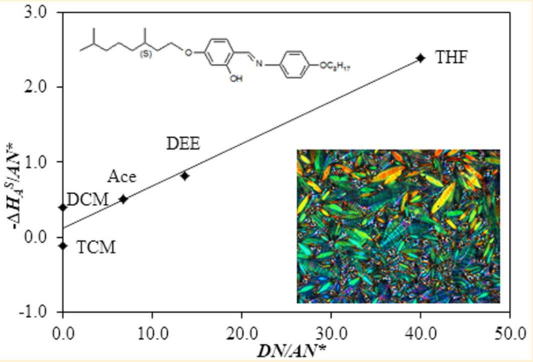

1. INTRODUCTION

Liquid crystals (LCs) which exhibit a combination of fluidity and long-range order are a fascinating class of soft materials with high technological importance.[1,2] These ordered soft materials are used in a wide variety of fields of advanced technologies such as electron, ion, molecular transporting, sensing, catalysis, as well as primarily LC display devices.[2,3] The mesogenic materials based on rodlike anisometric units show helical superstructures such as chiral smectics by introduction of chirality.[4,5] On the other hand, salicylimine linking groups are very useful to provide stability on mesomorphic properties due to intramolecular hydrogen bonding.[6]

The molecular shape in LCs is effective in the formation of mesophase. Calamitic LCs consist of a rigid core with at least two aromatic rings, which are covalently connected by linking groups and flexible terminal chains.[7] The various functional groups can be incorporated for certain material properties. For example salicylaldimines have been favorably employed in the LC synthesis to establish mesogenic complexes showing novel desirable physical properties by incorporating transition metal atoms to mesogenic ligands.[8]

One of the major aims in the design of LC materials is to understand the molecular interactions induced in the LC mesophases for developing suitable new applications. Salicylaldimine LCs are sufficiently sensitive to various external effects such as temperature, electric and magnetic fields, and deformation of surfaces.[9] Also, the synthetic ease and self-organizing abilities of salicylaldimines offer a viable option to obtain multifunctional materials. The characterization of surface and solubility properties of these materials provides striking benefits to realize electrostatic association, H-bonding, or donor−acceptor interactions and miscibility to enable the development of some applications such as sensitive chemical and biological sensors using LC-based materials.[10] The LCs also have the ability to separate the structural isomers from their mixtures if they are used as a stationary phase in a column. Thus, interaction data of LCs with various liquids are required in the separation techniques.

Received: October 8, 2018
Accepted: February 12, 2019

DOI: 10.1021/acs.jced.8b00903

Inverse gas chromatography (IGC) at infinite dilution is a useful and quite versatile technique applied for thermodynamical characterization of a wide range of systems such as polymers, LCs, composite materials, pharmaceutical solids, etc.[11−13] The term "inverse" indicates that the stationary phase of the chromatographic column is of interest, in contrast to conventional gas chromatography. The retention data were obtained by injection of some selected solvents called probes at suitable temperatures. The surface properties of the material in the column are determined from the retention data at lower temperatures while the solubility characteristics are determined from the retention data at the thermodynamical equilibrium region at higher temperatures.[14−16]

In this work, we determined the dispersive surface energy, acid and base constants, and solubility data at higher temperatures of a new chiral calamitic LC, DOPIMP, by using the IGC technique.

2. THEORETICAL BASIS

2.1. Surface Characterization. IGC is known as a reasonable technique to measure surface properties of the samples in the chromatographic column as a stationary phase,[17] and extensively applied for characterization of various materials.[15] Dispersive surface energy and acid−base constants of the solid material can be determined from the net retention volume, V_N given as

$$V_N = QJ_3^2(t_R - t_A)T/(T_f) \tag{1}$$

where Q is carrier gas flow, J_3^2 is the pressure correction factor term and is given by $J_3^2 = [3(p_i/p_0)^2 - 1]/[2(p_i/p_0)^3 - 1]$ where the inlet pressure is p_i and the outlet pressure is p_0, t_R and t_A are retention times of the solvent and air, respectively; T_f(K) and T(K) are temperatures of ambient and column, respectively.

Since the theoretical background is explained in detail in our previous works,[18−20] it is explained in summary in the present study. V_N is linked to the Gibbs free energy of adsorption (ΔG_A) of the solvents on the sample in the column;

$$\Delta G_A = -RT \ln(V_N) + K \tag{2}$$

where R is the universal gas constant and K is a constant related the reference state. ΔG_A is the sum of its two components, that is, dispersive (ΔG_A^D) and specific (acid−base) (ΔG_A^S). When n-alkanes are used as solvents, ΔG_A equals to ΔG_A^D because of the absence of specific interaction between n-alkanes and the sample in the column.[21]

In this case, ΔG_A is related to the dispersive components of surface energies of the sample, γ_S^D and n-alkanes, γ_L^D, respectively, as proposed by Schultz[22]

$$-\Delta G_A = -\Delta G_A^D = 2N_A a(\gamma_S^D \gamma_L^D)^{1/2} \tag{3}$$

where N_A is the Avogadro's number and a is the cross-sectional area of the solvent molecule.

On the other hand, Dorris and Gray[23] proposed to determine γ_S^D from the Gibbs free energy of adsorption increment per mole of methylene group ($\Delta G_{[CH_2]}$) using the relationship:

$$-\Delta G_{[CH_2]} = 2N_A a_{[CH_2]}(\gamma_S^D \gamma_{[CH_2]}^D)^{1/2} \tag{4}$$

where $a_{[CH_2]}$ is the surface area covered by one methylene group (0.06 nm^2) and $\gamma_{[CH_2]}^D$ is the dispersive surface energy of a surface consisting of only methylene groups, that is, polyethylene, given by, $[\gamma_{[CH_2]}^D = 35.6 + 0.058(293.2 - T)$ and $\Delta G_{[CH_2]}$ was obtained from the slope of the plot ΔG_A versus C atom numbers of the used n-alkanes.

The specific component of the Gibbs free energy of adsorption, $-\Delta G_A^S$ is related to the solid phase's ability to act as a donor (basic) or an acceptor (acidic) to the electrons. To determine acid and base constants of the sample, the ΔG_A^D values of the corresponding hypothetical n-alkanes are subtracted from ΔG_A of the used polar solvents. The distance between the ordinate values of the polar probes and the n-alkane reference line gives $-\Delta G_A^S$:

$$-\Delta G_A^S = RT \ln\left(\frac{V_{N,n}}{V_{N,ref}}\right) \tag{5}$$

where $V_{N,n}$ and $V_{N,ref}$ are the retention volumes for the polar solvent and the corresponding hypothetical n-alkane on their reference line, respectively.

ΔG_A^S results from specific components of the adsorption enthalpy (ΔH_A^S) and entropy (ΔS_A^S) between the examined surface and polar solvent:

$$\Delta G_A^S = \Delta H_A^S - T\Delta S_A^S \tag{6}$$

ΔH_A^S is related to the acidic or the basic character through the equation given by Gutmann:

$$-\Delta H_A^S = K_A(\mathrm{DN}) + K_D(\mathrm{AN}^*) \tag{7}$$

where DN and AN* are Gutmann's donor and modified acceptor numbers, respectively, whereas K_A and K_D are acid and base constants of the sample surface, respectively, which are indicators reflecting its Lewis acidity and basicity. Consequently, K_A and K_D can be determined by the slope and intercept, respectively, of the straight line obtained by plotting $-\Delta H_A^S/\mathrm{AN}^*$ versus DN/AN*. The ratio K_D/K_A provides an empirical basis for the classification of the surface with respect to acidity−basicity. The surface is considered to be basic if the ratio is higher than 1 or *vice versa.*

2.2. Solubility of the DOPIMP in the Solvents. If the stationary phase is in the molten state in the chromatography column, the measured retention data can be used to determine the mole fraction activity coefficients at infinite dilution, γ_{12}^∞, for the probe solvents by using the equations developed by Everett[24] and Cruickshank[25]

$$\ln \gamma_{12}^\infty = \ln\left(\frac{n_2 RT}{V_N p_1^0}\right) - \frac{p_1^0(B_{11} - V_1^0)}{RT} + \frac{p_0 J_2^3(2B_{13} - V_1^\infty)}{RT} \tag{8}$$

where n_2 is the number of moles of the nonvolatile material used as the stationary phase in the column, p_1^0, B_{11}, and V_1^0 are the saturated vapor pressure, gaseous state second virial coefficient, and molar volume of the solvent probe, respectively, at column temperature, T(K). B_{13} is the mixed second virial coefficient of the solvent probe and carrier gas. Guillett et al.[26] stated that the last term in eq 8 can be ignored at moderate carrier gas pressures (less than 202.65 kPa). In this case, eq 8 becomes

$$\ln \gamma_{12}^\infty = \ln\left(\frac{n_2 RT}{V_N p_1^0}\right) - \frac{p_1^0(B_{11} - V_1^0)}{RT} \tag{9}$$

DOI: 10.1021/acs.jced.8b00903
J. Chem. Eng. Data XXXX, XXX, XXX−XXX

Table 1. Purities and Purification Methods of the Reagents

chemical name	abbreviation	source	CASRN	initial mole fraction purity	purification method
(*S*)-(-)-*β*-citronellol		Aldrich	7540-51-4	≥0.99	none
palladium on carbon 10 wt. % loading (dry basis)		ALFA.A120120			none
methanol	MeOH	technical grade			distillation
hydrobromic acid	HBr	ABCR-AB203595		48%	none
sulfuric acid extra pure	H_2SO_4	Merck	7664-93-9	0.95−0.98	none
tetrabutylammonium hydrogen sulfate	TBAHS	Sigma-Aldrich	32503-27-8	≥0.97	none
2,4-dihydroxy benzaldehyde		Aldrich	95-01-2	≥0.98	none
potassium hydrogen carbonate	$KHCO_3$	Merck	298-14-6	ACS	none
N,*N*-dimethilformamid		Merck	68-12-2	ACS	none
p-toluenesulfonic acid monohydrate		Merck	6192-52-5		none
chloroform	TCM	Supelco	67-66-3	≥0.99	none
n-hexane	Hx	Supelco	110-54-3	≥0.99	none
n-heptane	Hp	Supelco	142-82-5	≥0.99	none
n-octane	O	Supelco	111-65-9	≥0.99	none
n-nonane	N	Sigma-Aldrich	111-84-2	≥0.99	none
n-decane	D	Sigma-Aldrich	124-18-5	≥0.99	none
undecane	UD	Merck	16416-29-8	≥0.99	none
ethyl acetate	EA	Supelco	141-78-6	≥0.998	none
n-butyl acetate	nBA	Supelco	123-86-4	≥0.995	none
iso-butyl acetate	iBA	Sigma-Aldrich	110-19-0	≥0.98	none
n-propylbenzene	nPB	Sigma-Aldrich	103-65-1	≥0.99	none
tetrahydrofurane	THF	Supelco	109-99-9	≥0.998	none
acetone	Ace	Supelco	67-64-1	≥0.998	none
diethyl ether	DEE	Supelco	60-29-7	≥0.997	none
dichloromethane	DCM	Supelco	75-09-2	≥0.995	none
ethylbenzene	EB	Sigma-Aldrich	100-41-4	≥0.99	none
chlorobenzene	CB	Sigma-Aldrich	108-90-7	≥0.995	none
toluene	T	Supelco	108-88-3	≥0.998	none

The values of γ_{12}^{∞} of a solvent probe for the liquid material used as stationary phase provide information related to their intermolecular interaction. The fact that γ_{12}^{∞} is equal to 1 indicates ideal mixing, while smaller and larger values than 1 show favorable and unfavorable interactions, respectively.

Since γ_{12}^{∞} contains all of the deviations from the ideality, the partial molar residual enthalpic $(\Delta \bar{H}_1^{E,\infty})$ and entropic $(\Delta \bar{S}_1^{E,\infty})$ components of the interaction at infinite dilution can be estimated from the slope and intercept of a straight line between logarithm of γ_{12}^{∞} and reciprocal of the absolute temperature according to eq 10

$$\ln \gamma_{12}^{\infty} = \frac{\Delta \bar{H}_1^{E,\infty}}{RT} - \frac{\Delta \bar{S}_1^{E,\infty}}{R} \tag{10}$$

3. EXPERIMENTAL METHODS

3.1. Materials and Instrumentations.

Chromosorb-W (AW-DMCS-treated, 80/100 mesh) support material was supplied from Merck AG Inc. Silane treated glass wool, used to plug the ends of the column, was obtained from Alltech Associates, Inc. Before measurements, we also confirmed that the column walls and Chromosorb W (AW-DMCS) and silanized glass wool did not adsorb any solvent.

A Hewlett-Packard 6890N model gas chromatograph with a thermal conductivity detector was used to measure the retention times of the solvents. The column was made of stainless steel tubing with 3.2 mm outside diameter and 1 m length. The LC was coated on the support by slow evaporation of TCM as stirring the Chromosorb W (AW-DMCS) in the LC solution. The amount of coated LC on the support was determined as 9.15% by calcination. A trace amount of solvent was injected into the chromatograph by injecting the air filled up after all of the small amount solvent in the micropipette is discharged into the air. Before the experiments, it was determined that the retention time does not depend on the sample size and flow rate of the carrier gas and eluted peaks are sharp and reproducible. The column was conditioned at 373 K for 24 h under a helium atmosphere. Transition temperatures were measured, and optical investigations were carried out using a Mettler FP-82 HT hot stage and a control unit in conjunction with a Leica DM2700P polarizing microscope and Leica DMC2900 digital camera. The associated enthalpies were obtained from DSC-thermograms which were recorded on a Perkin-Elmer DSC-7 with a heating and cooling rate of 10 °C min^{-1}. The purity of reagents and their purification methods are given in Table 1.

3.2. Synthesis and Characterization of DOPIMP.

DOPIMP was synthesized according to the procedure described previously in the literature.[27−29] (*S*)-(-)-*β*-Citronellol was reduced to (*S*)-3,7-dimethyl-1-octanol under catalytic hydrogenation conditions (H_2, 10% Pd/C in MeOH) in the first reaction step of the DOPIMP. Then, (*S*)-3,7-dimethyloctyl bromide was prepared from (*S*)-3,7-dimethyl-1-octanol by reaction with 48% aq HBr/concn H_2SO_4 using TBAHS as catalyst.[30] The aldehyde carrying the (*S*)-3,7-dimethyloctyloxy group was obtained by the reaction of 2,4-dihydroxybenzaldehyde with (*S*)-3,7-dimethyloctyl bromide, using $KHCO_3$ as base in DMF solvent. Finally, the condensation of the 4-((*S*)-3,7-dimethyloctyloxy)-2-hydroxybenzaldehyde and 4-(octyloxy)aniline in T using *p*-toluenesulfonic acid monohydrate as catalyst yields new salicylaldimine-based chiral calamitic LC, DOPIMP.[31] Spectroscopic data and mesomorphic properties for the DOPIMP LC were given in Mutlu Yanic et al..[31]

The phase transition temperatures and chemical structure of DOPIMP are shown in Figure 1.

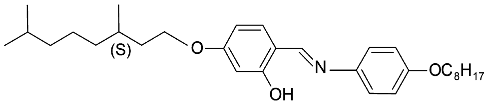

Compound	t/°C [ΔH kJ mol⁻¹]
DOPIMP[31]	Cr1 33 [8.06] Cr2 39 [3.55] SmC* 88 [4.44] Iso

Figure 1. Chemical structure and phase transition temperatures *t* (°C) and enthalpies ΔH [kJmol^{-1}] of DOPIMP (Perkin-Elmer DSC-7; heating rates 10 °C min^{-1}; abbrevations, Cr = crystalline, SmC* = chiral smectic C phase, Iso = isotropic liquid phase).

The salicylaldimine-based chiral calamitic LC with a (*S*)-3,7-dimethyloctyloxy group at one of the terminals, DOPIMP, exhibits enantiotropic chiral smectic C* mesophase in a wide temperature range. When the LC was cooled from the isotropic liquid, the fingerprint texture of Cr and SmC* phase was observed under the polarizing microscope as shown in Figure 2a,b.

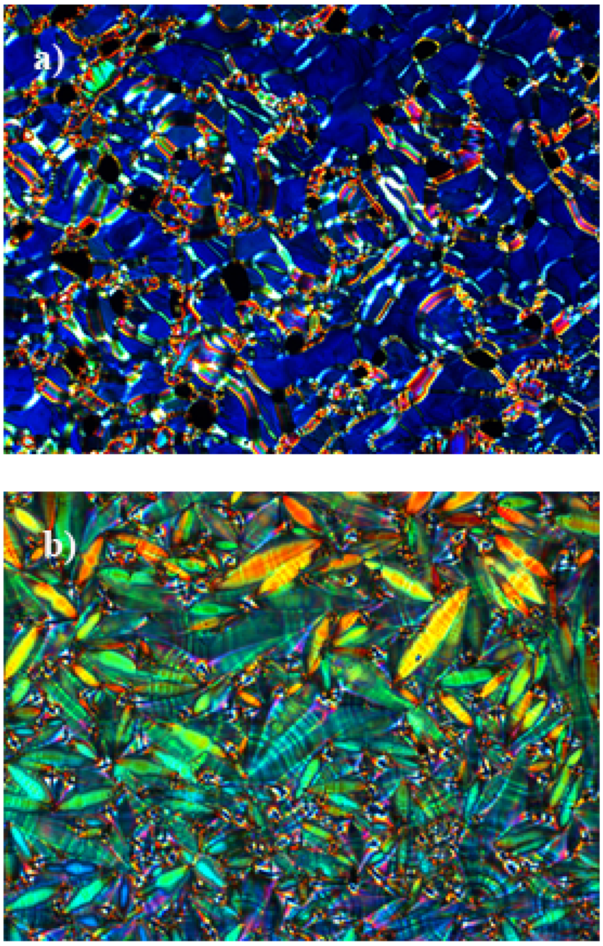

Figure 2. Texture of the Cr and SmC* phase obtained between crossed polarizers at 35 °C (a) and 60 °C (b) on cooling.

4. RESULTS AND DISCUSSION

4.1. Surface Characterization of DOPIMP. At first, the retention data were recorded at the temperatures between room temperature and 125 °C in order to see the thermal transition points if any. A transition point at 57 °C was detected in the retention diagram drawn between ln V_N versus $1/T$, belonging to the crystalline-SmC* transition. Detection of a different transition temperature in the IGC test compared to DSC is common since the measured properties and experimental conditions of these two techniques are quite different. DSC measures the heat taken or given by the substance, whereas IGC measures the retention time of the sorbed probe molecules. In addition, DSC is a dynamic technique but IGC is a static technique. The retention data at the thermodynamic equilibrium region for which the variation is a straight line should be used to obtain accurate results.

The adsorption properties of the DOPIMP surface were investigated by IGC technique between 303.2 and 328.2 K at the thermodynamic equilibrium absorption region which was linear straight lines as seen in Figures 3 and 4. The net retention volumes, V_N, were obtained by the retention times which were precise and reproducible to ± 0.01 min according to the eq 1.

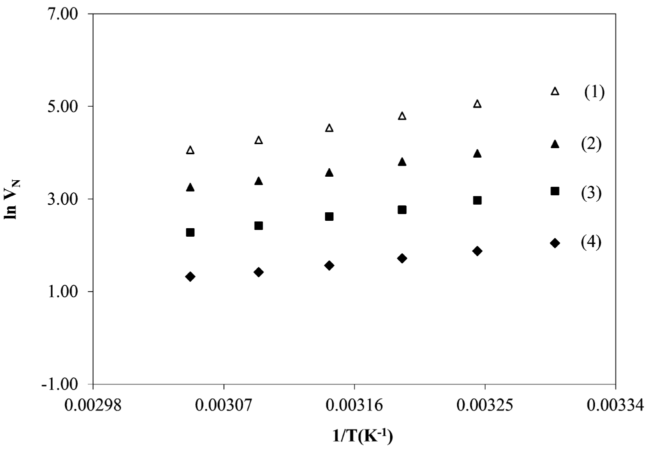

Figure 3. Net retention volumes V_N of nonpolar solvents: N (1), O (2), Hp (3), and Hx (4).

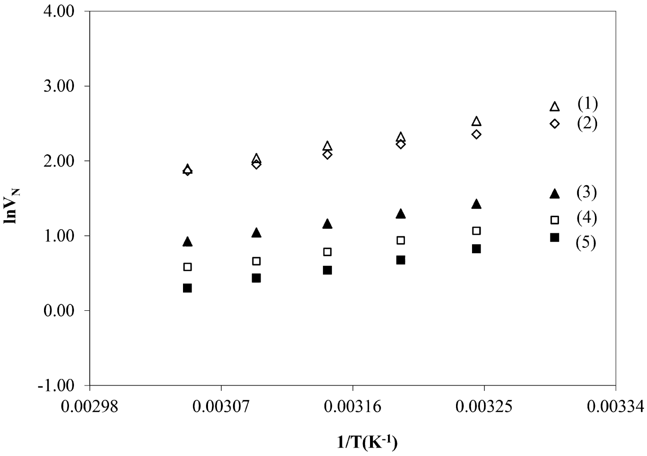

Figure 4. Net retention volumes V_N of polar solvents: THF (1), TCM (2), DCM (3), Ace (4), and DEE (5).

Using eqs 1−5, a dispersive component of the surface energy γ_S^D of DOPIMP was calculated by the methods of Schultz and Doris-Gray. The details of the methods were given in our earlier papers.[32,33] The obtained γ_L^D values were given in a linear line with their corresponding regression coefficients at a temperature range from 303.2 to 328.2 K.

$$\text{Schultz:} \quad \gamma_S^D/\text{mJ m}^{-2} = 40.8 - 0.273\ (T/\text{K},\ 303.2) \quad R^2 = 0.988$$

$$\text{Dorris-Gray:} \quad \gamma_S^D/\text{mJ m}^{-2} = 41.4 - 0.215\ (T/\text{K},\ 303.2) \quad R^2 = 0.975$$

It can be seen that there is not much discrepancy between the values obtained from these two methods. The dispersive surface energy of DOPIMP can be accepted as 41.1 mJ m^{-2} at 30 °C as a mean of the values found from these methods. This value is in agreement with the values of LCs reported as about 40 mJ m^{-2} in the literature.[18,33]

The acid−base characterization was implemented by means of ΔG_A^S which is the difference between the Gibbs free energies of adsorption of polar and nonpolar probes. Then, ΔH_A^S of polar probes was obtained from the slope of the straight line of $-\Delta G_A^S/T$ against $1/T$. The values of ΔH_A^S were specified as the degree of interaction between the surface of DOPIMP and the selected polar solvents.

A plot of $-\Delta H_A^S$/AN* versus DN/AN* was drawn with K_A as the slope and K_D as the intercept using eq 7, and it is shown in Figure 5. The obtained K_A and K_D are found to be 0.056 ± 0.014 and 0.118 ± 0.010, respectively. The ratio of K_D/K_A (=2.1) suggests that the surface of DOPIMP has a basic character at temperatures between 303.2 and 328.2 K. This can be attributed to a lone pair of electrons on the nitrogen atom of the DOPIMP structure.

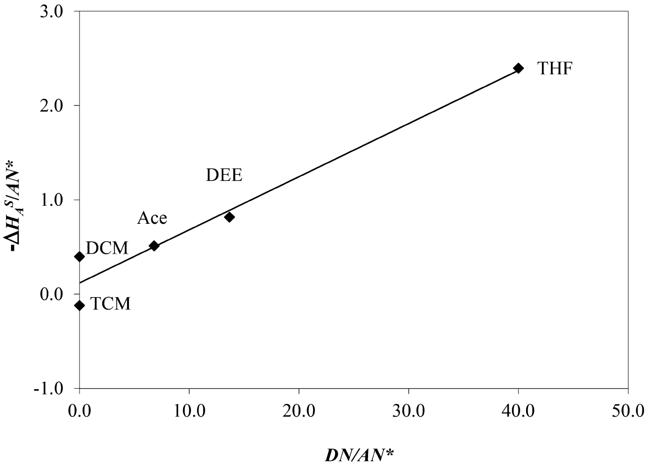

Figure 5. Plot of $-\Delta H_A^S$/AN* versus DN/AN*.

4.2. Solubility of DOPIMP. The net retention volumes, V_N of the solvents such as Hx, Hp, O, N, D, UD, CB, EB, nBA, T, IBA, and EA on the liquid state DOPIMP were determined by using eq 1 at temperatures between 368.2 and 398.2 K. The percentage errors in V_N were not higher than ±0.3 using four or five consecutive measurements of each data. The linearity of the plots in Figures 6 and 7 indicates that a thermodynamic equilibrium region is attained. It means that reasonable thermodynamic data related to the solubility of DOPIMP can be obtained at the region between 368.2 and 398.2 K.

It can be seen from the retention diagram in the Figure 7 that DOPIMP can be used as a stationary phase to separate the isomers of butyl acetates, that is, nBA and IBA, from their mixtures by gas chromatography since their net retention volumes are quite different.

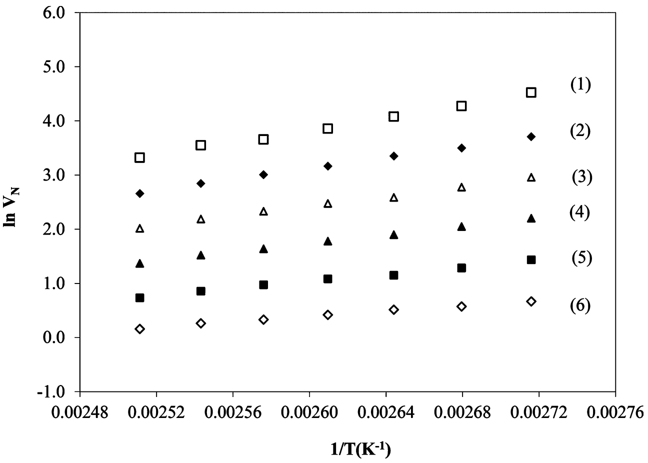

Figure 6. Net retention volumes, V_N, of UD (1), D (2), N (3), O (4), Hp (5), and Hx (6) on DOPIMP.

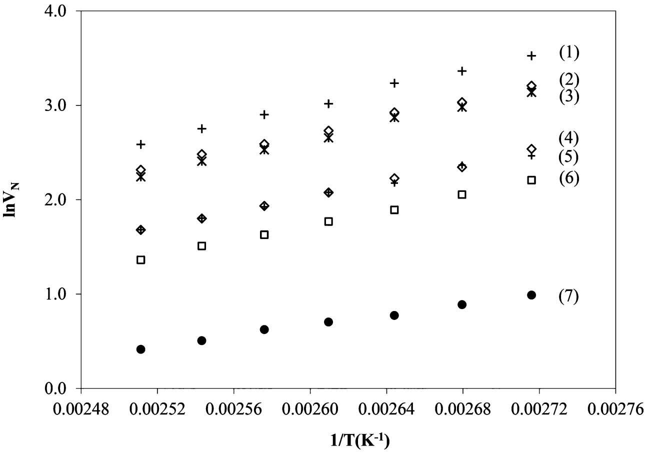

Figure 7. Net retention volumes, V_N, of nPB (1), CB (2), EB (3), nBA (4), T (5), IBA (6), and EA (7) on DOPIMP.

The mole fraction activity coefficient of the probe solvents at infinite dilution γ_{12}^∞ were obtained from eq 9 and their values were given in Table 2. The values of B_{11}, V_1^0, and p_1^0 of the probe solvents were estimated by means of the data given in the literature.[34]

It can be seen obviously that the values of γ_{12}^∞ decrease considerably with increasing chain length of *n*-alkanes. It can be stated that the mixture of DOPIMP with *n*-octane represents almost ideal behavior at 388.2 K since γ_{12}^∞ equals to 0.974. The data denote that the solubility of DOPIMP increases considerably with molar mass and eventually the best one is UD among the studied solvents. This implies that the dominant interaction is through the long alkyl tails of DOPIMP. This is also confirmed by increasing the solubility of the aromatic hydrocarbons as the chain length of their alkyl groups increases.

It can be stated from the Table 2 that there is a specific attractive interaction between the chlorine group of CB and DOPIMP since the values of γ_{12}^∞ decrease considerably with the introduction of chlorine group instead of methyl group of T. The increase of γ_{12}^∞ with temperature indicates the exothermic solubility of DOPIMP in the studied probe solvents.

DOI: 10.1021/acs.jced.8b00903
J. Chem. Eng. Data XXXX, XXX, XXX−XXX

Table 2. Values of the Mole Fraction Activity Coefficients at Infinite Dilution (γ_{12}^{∞}) of the Probe Solvents for DOPIMP at Different Temperatures[a]

	$(\gamma_{12}^{\infty})\times10^2$						
T(K)	368.2	373.2	378.2	383.2	388.2	393.2	398.2
$p_i - p_0$ (kPa)	76.96	80.07	80.40	80.39	81.95	83.77	84.51
solvent							
Hx	734	938	1150	1470	1840	2270	2880
Hp	140	191	258	322	420	549	718
O	27.5	38.4	53.4	71.5	97.4	129	176
N	5.63	8.24	12.1	16.3	22.6	31.2	44.1
D	1.18	1.80	2.58	3.81	5.45	7.78	11.3
UD	0.233	0.379	0.578	0.902	1.37	1.88	2.88
EA	4.21	5.48	7.19	8.99	11.3	14.7	18.6
IBA	34.6	48.5	68.2	91.9	125	166	226
nBA	18.6	27.2	36.8	51.2	70.3	95.2	127
nPB	2.50	3.60	4.97	7.46	10.1	13.9	19.6
EB	7.77	10.9	14.6	21.6	29.1	38.7	53.7
T	40.8	53.3	76.0	98.4	134	176	231
CB	8.37	11.9	15.9	22.9	31.1	40.8	56.4

[a] Standard uncertainties u are as follows: $u(\gamma_{12}^{\infty}) = 0.05$; $u(T) = 0.1$ K, $u(\bar{p}) = 0.07$ kPa.

The residual partial molar heat, $\Delta\bar{H}_1^{E,\infty}$ and residual partial molar entropy, $\Delta\bar{S}_1^{E,\infty}$ of mixing were determined from the slope and intercept, of the plot $\ln\gamma_{12}^{\infty}$, versus $1/T$, respectively, according to eq 10, and their values were given in Table 3. The negative values of $\Delta\bar{H}_1^{E,\infty}$ for all of the studied solvents refer to the exothermic solubility. It can be seen that all the residual thermodynamic parameters ($\Delta\bar{G}_1^{E,\infty}$, $\Delta\bar{H}_1^{E,\infty}$ and $\Delta\bar{S}_1^{E,\infty}$) have a negative sign and their absolute values increase with the increasing solubility, that is, the smaller is the γ_{12}^{∞} value, the higher is the absolute value of the residual thermodynamic parameters. The negative sign of $\Delta\bar{H}_1^{E,\infty}$ refers to favorable interactions between DOPIMP and probe solvents at infinite dilution. The negatively signed $\Delta\bar{S}_1^{E,\infty}$ implies that the probe solvents make the DOPIMP more regular. However, since the enthalpic contribution is higher than entropic contribution, the values of Gibbs energy become negative for all of the probe solvents except to Hx, Hp and EA.

Table 3. Values of Partial Molar Residual Gibbs Energy ($\Delta\bar{G}_1^{E,\infty}$), Enthalpy ($\Delta\bar{H}_1^{E,\infty}$), and Entropy ($\Delta\bar{S}_1^{E,\infty}$) of the Probe Solvents for DOPIMP at 368.2 K

	$-\Delta\bar{H}_1^{E,\infty}$ (kJ/mol)	$-\Delta\bar{S}_1^{E,\infty}$ (kJ/mol K)	$-\Delta\bar{G}_1^{E,\infty}$ (kJ/mol)
Hx	55.1	0.166	−6.08
Hp	65.2	0.181	−1.07
O	74.8	0.193	3.94
N	82.4	0.200	8.76
D	91.1	0.210	13.6
UD	101	0.224	18.5
nBA	77.7	0.197	5.06
IBA	75.8	0.197	3.22
EA	60.1	0.175	−4.40
nPB	83.4	0.196	11.3
EB	75.5	0.192	7.85
ClB	77.1	0.189	7.58
T	71.0	0.185	2.79

5. CONCLUSIONS

The dispersive surface energy, γ_S^D of DOPIMP was found as 41.1 mJ/m^2 at 30 °C by averaging the values found from the methods proposed by Schultz and Dorris−Gray and decreased with temperature. The value of K_D/K_A (=2.1) suggests that the surface of DOPIMP has somewhat basic character. DOPIMP can be used as a stationary phase to separate the nBA and IBA from their mixtures by gas chromatography.

The mole fraction activity coefficients of the probe solvents at infinite dilution, (γ_{12}^{∞}) suggest that among the studied probe solvents, UD is the best one for DOPIMP. The probe solvents can be sorted according to their decreasing power as UD > D > nPB > EA > N > EB > CB > nBA > O > *T* > Hp > Hx. All the studied solvents show exothermic solubility behavior.

It can be concluded that IGC is a convenient method to obtain quantitative data related to surface energetics and solubility of a LC in various solvents to use in convenient designs in new application fields.

■ ASSOCIATED CONTENT

Supporting Information

The Supporting Information is available free of charge on the ACS Publications website at DOI: 10.1021/acs.jced.8b00903.

Characterization of the DOPIMP based on ^{1}H-, ^{13}C NMR (PDF)

■ AUTHOR INFORMATION

Corresponding Author

*E-mail: kurtaran90@yahoo.com.

ORCID

Fatih Cakar: 0000-0001-6192-1370
Ozlem Cankurtaran: 0000-0002-8383-1170

Funding

This research has been supported by Scientific Research Projects Coordination Center of Yildiz Technical University, Turkey (2015-01-02-DOP01).

Notes

The authors declare no competing financial interest.

■ REFERENCES

(1) Lagerwall, J. P. F.; Scalia, G. A new era for liquid crystal research: Applications of liquid crystals in soft matter nano-, bio- and microtechnology. *Curr Appl Phys* **2012**, *12*, 1387−1412.

(2) Kato, T.; Mizoshita, N.; Kishimoto, K. Functional liquid-crystalline assemblies: Self-organized soft materials. *Angew. Chem., Int. Ed.* **2006**, *45*, 38−68.

(3) Bisoyi, H. K.; Kumar, S. Liquid-crystal nanoscience: an emerging avenue of soft self-assembly. *Chem. Soc. Rev.* **2011**, *40*, 306−319.

(4) Tschierske, C. Liquid crystal engineering − new complex mesophase structures and their relations to polymermorphologies, nanoscale patterning and crystal engineering. *Chem. Soc. Rev.* **2007**, *36*, 1930−1970.

(5) Kitzerow, H. S.; Bahr, C. *Chirality in Liquid Crystals*; Springer-Verlag: New York, 2001.

(6) Ocak, H.; Bilgin-Eran, B.; Tschierske, C.; Baumeister, U.; Pelzl, G. Effect of fluorocarbon chains on the mesomorphic properties of chiral imines and their complexes with copper(II). *J. Mater. Chem.* **2009**, *19*, 6995−7001.

(7) Goodby, J. W.; Collings, P. J.; Kato, T.; Tschierske, C.; Gleeson, H.; Raynes, P. Fundamentals of Liquid Crystals. *Handbook of Liquid Crystals*, 2nd ed.; Wiley-VCH: Weinheim, Germany, 2014; Vol *1*.

(8) Hoshino, N. Liquid crystal properties of metal−salicylaldimine complexes. Chemical modifications towards lower symmetry. *Coord. Chem. Rev.* **1998**, *174*, 77−108.

(9) Nesrullajev, A.; Bilgin Eran, B. Study of mesomorphism, thermotropic properties and pitch in new chiral smectogenic imine compounds. *J. Mol. Liq.* **2015**, *209*, 25−32.

(10) Xiaokang, D.; Kun-Lin, Y. Liquid crystal based optical sensor for detection of vaporous butylamine in air. *Sens. Actuators, B* **2012**, *173*, 607−613.

(11) Corpart, J. M.; Girault, S.; Juhue, D. Structure and surface properties of liquid crystalline fluoroalkyl polyacrylates: Role of the spacer. *Langmuir* **2001**, *17*, 7237−7244.

(12) Boudriche, L.; Hamdi, B.; Kessaissia, Z.; Calvet, R.; Chamayou, A.; Dodds, J. A.; Balard, H. An assessment of the surface properties of milled attapulgite using inverse gas chromatography. *Clays Clay Miner.* **2010**, *58*, 143−153.

(13) Shillcock, I. M.; Price, G. J. Inverse gas chromatography study of poly(dimethyl siloxane)-liquid crystal mixtures. *Polymer* **2003**, *44*, 1027−1034.

(14) Shi, B.; Wang, Y.; Jia, L. Comparison of Dorris−Gray and Schultz Methods for the calculation of surface dispersive free energy by inverse gas chromatography. *J Chromatogr A* **2011**, *1218*, 860−862.

(15) Benkacem, T.; Hamdi, B.; Chamayou, A.; Balard, H.; Calvet, R. Physicochemical characterization of a diatomaceous upon an acid treatment: a focus on surface properties by inverse gas chromatography. *Powder Technol.* **2016**, *294*, 498−507.

(16) Uhlmann, P.; Schneider, S. Acid−base and surface energy characterization of grafted polyethylene using inverse gas chromatography. *J Chromatogr A* **2002**, *969*, 73−80.

(17) Adamska, K.; Voelkel, A.; Berlinska, A. The solubility parameter for biomedical polymers-application of inverse gas chromatography. *J. Pharm. Biomed. Anal.* **2016**, *127*, 202−206.

(18) Ocak, H.; Mutlu Yanic, S.; Cakar, F.; Bilgin Eran, B.; Guzeller, D.; Karaman, F.; Cankurtaran, O. A study of the thermodynamical interactions with solvents and surface characterisation of liquid crystalline 5-((S)-3,7-dimethyloctyloxy)-2-[[[4-(dodecyloxy) phenyl] imino]-methyl]phenol by inverse gas chromatography. *J. Mol. Liq.* **2016**, *223*, 861−867.

(19) Cakar, F.; Ocak, H.; Ozturk, E.; Mutlu-Yanic, S.; Kaya, D.; San, N.; Cankurtaran, O.; Bilgin-Eran, B.; Karaman, F. Investigation of thermodynamic and surface characterisation of 4-[4-(2-ethylhexyloxy)benzoyloxy]benzoic acid thermotropic liquid crystal by inverse gas chromatography. *Liq. Cryst.* **2014**, *9*, 1323−1331.

(20) Ocak, H.; Sakar, D.; Cakar, F.; Cankurtaran, O.; Bilgin-Eran, B.; Karaman, F. Use of inverse gas chromatography for the physicochemical characterisation of a new synthesised liquid crystal: (S)-5-(2-methylbutoxy)-2-{[(4-dodecyloxyphenyl)imino]methyl}-phenol. *Liq. Cryst.* **2008**, *12*, 1351−1358.

(21) Karakehya, N.; Bilgic, C. Surface characterisation of montmorillonite/PVC nanocomposites by inverse gas chromatography. *Int. J. Adhes. Adhes.* **2014**, *51*, 140−147.

(22) Hamieh, T.; Schultz, J. New approach to characterise physicochemical properties of solid substrates by inverse gas chromatography at infinite dilution: I. Some new methods to determine the surface areas of some molecules adsorbed on solid surfaces. *J Chromatogr A* **2002**, *969*, 17−25.

(23) Dorris, G. M.; Gray, D. G. Adsorption of n-alkanes at zero surface coverage on cellulose paper and wood fibres. *J. Colloid Interface Sci.* **1980**, *77*, 353−362.

(24) Everett, D. H. Effect of Gas Imperfection on G.L.C. Measurements: A refined method for determining activity coefficients and second virial coefficients. *Trans. Faraday Soc.* **1965**, *61*, 1637−1645.

(25) Cruickshank, A. J. B.; Gainey, B. W.; Hicks, C. P.; Letcher, T. M.; Moody, R. W.; Young, C. L. Gas-liquid chromatographic determination of cross-term second virial coefficients using glycerol. Benzene + nitrogen and benzene + carbon dioxide at 50°C. *Trans. Faraday Soc.* **1969**, *65*, 1014−1031.

(26) Guillet, J. E.; Romansky, M.; Price, G. J.; Mark, R. V. D. *Inverse Gas Chromatography, Characterization of Polymers and Other Materials*; ACS Symposium Series; American Chemical Society: Washington, DC, 1989; Chapter 3.

(27) Bilgin-Eran, B.; Ocak, H.; Tschierske, C.; Baumeister, U. Synthesis and mesomorphism of fluoroalkylated platinum complexes. *Liq. Cryst.* **2012**, *39*, 467−476.

(28) Bilgin-Eran, B.; Tschierske, C.; Diele, S.; Baumeister, U. Synthesis and mesomorphism of fluoroalkylated organometallic mesogens. *J. Mater. Chem.* **2006**, *16*, 1136−1144.

(29) Nesrullajev, A.; Bilgin-Eran, B. Study of mesomorphism, thermotropic properties and pitch in new chiral smectogenic imine compounds. *J. Mol. Liq.* **2015**, *209*, 25−32.

(30) Guzeller, D.; Ocak, H.; Bilgin-Eran, B.; Prehm, M.; Tschierske, C. Development of tilt, biaxiality and polar order in bent-core liquid crystals derived from 4′-hydroxybiphenyl-3-carboxylic acid. *J. Mater. Chem. C* **2015**, *3*, 4269−4282.

(31) Mutlu Yanic, S.; Ocak, H.; Cakar, F.; Bilgin-Eran, B.; Güzeller, D.; Cankurtaran, O. Morphology and preparation of polymer dispersed liquid crystals by solvent-induced phase separation method. *Optoelectron. Adv. Mater.* **2017**, *11* (1−2), 77−81.

(32) Eken Korkut, S.; Yazici, O.; Cakar, F. Surface and thermodynamic characterizations and secondary transition of novel phthalocyanine glass. *J. Chem. Eng. Data* **2018**, *63*, 1146−1153.

(33) Erol, I.; Cakar, F.; Ocak, H.; Cankurtaran, H.; Cankurtaran, O.; Bilgin Eran, B.; Karaman, F. Thermodynamic and surface characterisation of 4-[4-((S)-citronellyloxy) benzoyloxy] benzoic acid thermotropic liquid crystal. *Liq. Cryst.* **2016**, *43*, 142−151.

(34) Poling, B. E.; Prausnitz, J. M.; O'Connell, J. P. *The properties of gases and liquids*; McGraw-Hill Companies, Inc.: 2001.

DOI: 10.1021/acs.jced.8b00903
J. Chem. Eng. Data XXXX, XXX, XXX−XXX